

## Level set segmentation method in cancer's cells images

Ali Elyasi\*†, Yousef Ganjdanesh\*\*, Kave Kangarloo\*, Mehdi Hossini\*\*, Marzie Esfandyari\*\*

\*Department of Electrical Engineering, Islamic Azad University Central Tehran Branch, Poonak Sq. Tehran, Iran

\*\*Department of Electrical Engineering, Islamic Azad University Saveh Branch, Felestin Sq. Saveh, Iran

†Corresponding Author: Tel:+98 21 66423022, E-mail: [alielyasi15@gmail.com](mailto:alielyasi15@gmail.com)

**Abstract:** For early detection in cancer, it is necessary that cells be monitored on time. One of the first steps in the monitoring process is segmenting the cancer's cells. In this paper, we focused on the level set method and compared with snake active contour that use in image segmentation. Level set method is a fast and accurate approach that can be used in segmentation and reduce human interaction as possible. A set of cancer cells images is selected to serve as the representative test set. The selections are different sizes and resolutions.

[Ali Elyasi, Yousef Ganjdanesh, Kave Kangarloo, Mehdi Hossini. Level set segmentation method in cancer's cells images. Journal of American Science 2011;7(2):196-204]. (ISSN: 1545-1003). <http://www.americanscience.org>.

Keywords: Level set; GVF snake; cancer's cell; Image segmentation;

### Introduction:

Medical imaging allows scientist and physicians to decide about life saving information regard to the human physiological activities. It plays an important role in the diagnosis, therapy and treatment of various organs, tumors and other abnormalities. Image segmentation is typically used to locate objects and boundaries in images and should stop when the object of interest in an application have been isolated. It is used to calculate the geometric shape and size of tumors and abnormal growth of any tissue. There are many techniques available for auto-segmentation of images like Active contours [13, 14], Fuzzy based classifiers [16], Gradient Vector Field theory, Tensor based segmentation, Level set theory etc. But many of them are suffering from problems like optimization, initialization and insufficient results in noisy images. Most widely used segmentation is level set segmentation in biomedical medical images [15] such as X-ray, CT and MRI. The level set technique or active contour is a powerful numerical technique for image processing. A predecessor to the level set methods: Level set method was first introduced by Osher and Sethian [1] that it is an implicit (non-parametric) technique and introduced in the medical vision community by malladi et al.[2], the active contour snakes [3] used parameterized representation of curves to segment images[3]. The geodesic active contours [17] had an added advantage of handling changing topology of the evolving curve implicitly,

but could only use boundary information, such as image gradients. The region competition algorithm [18] introduced a way of incorporating statistical region based information to evolve curves. But the Gaussian distribution specifically assumed for each region could prove restrictive in many cases. The active contours without edges method [19] provides a robust way of taking into account region information, including textures. However, the method is expected to perform unsatisfactorily whenever intensity distributions of the regions have the same first order moment but different higher order moments. The geodesic active contour method [4] unifies boundary and region based information along lines similar to those separately proposed in [17, 18] and so on. Since level set introduction, by Osher and Sethian [1], it has become a popular numerical method for the purpose of capturing the evolution of moving interfaces. In its simplest form, the method is very elegant, and offers some significant advantages over other interface tracking/capturing methods. Probably the most appealing feature of the method is its ability to handle changes in topology without complicated mesh generation, surface reconstruction, or collision detection. Particularly when considering applications in three dimensions or higher, this becomes a significant advantage: some other methods do not generalize so easily to higher dimensions. Another appealing feature of the level set method, which is often over looked, is its ties to numerical methods derived for hyperbolic conservation laws. This

connection allows the method to capture corners and cusps in the interface properly without non-physical loops and oscillations. Level set has been applied in many fields like physics , chemistry ,fluid mechanics , image processing , computer Vision and a collection of other areas .its applications cover most fields in image processing ,such as noise removal , image in painting , image segmentation and reconstruction that one of the critical problems in computer vision and image analysis is segmentation. Image segmentation plays a central role in numerous useful applications such as satellite image analysis, biomedical image processing, scene interpretation, video image analysis, content-based image database retrieval, and many others. For early detection in cancer it is necessary that cells be monitored on time.one of the first steps in the monitoring process is segmenting the cancer's cells .While this can be done manually, the process can be time consuming . Level set method be a fast and accurate approach that can be used in segmentation and reduce human interaction as possible.

**Gradient Vector Flow (GVF)**

This approach is external force model for active contours and deformable surfaces, which we called the gradient vector flow (GVF) field [5]. The field is calculated as a diffusion of the gradient vectors of a gray-level or binary edge map. It allows for flexible initialization of the snake or deformable surface and encourages convergence to boundary concavities .we define the gradient vector flow field to be the vector field  $V(x, y) = [u(x, y), v(x, y)]$  that minimizes the energy functional:

$$E = \int \mu(u_x^2 + u_y^2 + v_x^2 + v_y^2) + |\nabla f|^2 |V - \nabla f|^2 dx dy \tag{1}$$

This variation formulation follows a standard principle that of making the result smooth when there is no data. In particular, we see that when  $|\nabla f|$  is small; the energy is dominated by sum of the squares of the partial derivatives of the vector field, yielding as lowly varying field. On the other hand, when  $|\nabla f|$  is large, the second term dominates the integrand, and is minimized by setting  $V = \nabla f$  . This produces the desired effect of keeping V nearly equal to the gradient of the edge map when it is large , but forcing the field to be slowly varying in homogeneous regions. The parameter  $\mu$  is a regularization parameter governing the tradeoff between the first term and the second term in the integrand. This parameter should be set according to the amount of

noise present in the image (more noise, increase  $\mu$  ).We note that the smoothing term the first term with in the integrand of (1) is the same term used by Horn and Schunck in their classical formulation of optical flow [9]. It has recently been shown that this term corresponds to an equal penalty on the divergence and curl of the vector field [9]. Therefore, the vector field resulting from this minimization can be expected to be neither entirely irrational nor entirely solenoidal. Using the calculus of variations [10], it can be shown that the GVF field can be found by solving the following Euler equations.

$$\mu \nabla^2 u - (u - f_x)(f_x^2 + f_y^2) = 0 \tag{2a}$$

$$\mu \nabla^2 v - (v - f_y)(f_x^2 + f_y^2) = 0 \tag{2b}$$

Where  $\nabla^2$  is the Laplacian operator. These equations provide further intuition behind the GVF formulation. We note that in a homogeneous region [ where I (x,y) is constant ], the second term in each equation is zero because the gradient of f(x , y) is zero .Therefore , within such a region , u and v are each determined by Laplace’s equation , and the resulting GVF field is interpolated from the region’s boundary , reflecting a kind of competition among the boundary vectors . This explains why GVF yields vectors that point into boundary concavities. Equations (2a) and (2b) can be solved by treating u and v as functions of time and solving

$$u_t(x, y, t) = \mu \nabla^2 u(x, y, t) - [u(x, y, t) - f_x(x, y)] \cdot [f_x(x, y)^2 + f_y(x, y)^2] \tag{3a}$$

$$v_t(x, y, t) = \mu \nabla^2 v(x, y, t) - [v(x, y, t) - f_y(x, y)] \cdot [f_x(x, y)^2 + f_y(x, y)^2] \tag{3b}$$

The steady-state solution of these linear parabolic equations is the desired solution of the Euler equations (2a) and (2b). Note that these equations are decoupled, and therefore can be solved as separate scalar partial differential equations in u and v .The equations in (3) are known as generalized diffusion equations, and are known to arise in such diverse fields as heat conduction, reactor physics, and fluid flow [11]. Here, they have appeared from our description of desirable properties of snake external

force fields as represented in the energy functional of (1). For convenience, we write (3) as follows:

$$u_t(x, y, t) = \mu \nabla^2 u(x, y, t) - b(x, y)u(x, y, t) + c^1(x, y) \tag{4a}$$

$$v_t(x, y, t) = \mu \nabla^2 v(x, y, t) - b(x, y)v(x, y, t) + c^2(x, y) \tag{4b}$$

Where

$$b(x, y) = f_x(x, y)^2 + f_y(x, y)^2$$

$$c^1(x, y) = b(x, y)f_x(x, y)$$

$$c^2(x, y) = b(x, y)f_y(x, y)$$

Any digital image gradient operator [7] can be used to calculate  $f_x$  and  $f_y$ . To setup the iterative solution, let the indices  $i, j$ , and  $n$  correspond to  $x, y$ , and  $t$ , respectively, and let the spacing between pixels be  $\Delta x$  and  $\Delta y$  and the time step for each iteration be  $\Delta t$ . Then the required partial derivatives can be approximated as

$$u_t = \frac{1}{\Delta t} (u_{i,j}^{n+1} - u_{i,j}^n)$$

$$v_t = \frac{1}{\Delta t} (v_{i,j}^{n+1} - v_{i,j}^n)$$

$$\nabla^2 u = \frac{1}{\Delta x \Delta y} (u_{i+1,j} + u_{i,j+1} + u_{i-1,j} + u_{i,j-1} - 4u_{i,j})$$

$$\nabla^2 v = \frac{1}{\Delta x \Delta y} (v_{i+1,j} + v_{i,j+1} + v_{i-1,j} + v_{i,j-1} - 4v_{i,j})$$

Substituting these approximations into (4) gives our iterative solution to GVF as follows:

$$u_{i,j}^{n+1} = (1 - b_{i,j} \Delta t) u_{i,j}^n + r(u_{i+1,j}^n + u_{i,j+1}^n + u_{i-1,j}^n + u_{i,j-1}^n - 4u_{i,j}^n) + c_{i,j}^1 \Delta t \tag{5a}$$

$$v_{i,j}^{n+1} = (1 - b_{i,j} \Delta t) v_{i,j}^n + r(v_{i+1,j}^n + v_{i,j+1}^n + v_{i-1,j}^n + v_{i,j-1}^n - 4v_{i,j}^n) + c_{i,j}^2 \Delta t \tag{5b}$$

Where

$$r = \frac{\mu \Delta t}{\Delta x \Delta y} \tag{6}$$

Convergence of the above iterative process is guaranteed by a standard result in the theory of numerical methods. Provided that,  $c^1, c^2$  and are bounded, (5) is stable whenever the Courant – Friedrichs–Lewy step–size restriction  $r \leq \frac{1}{4}$  is maintained. Since normally  $\Delta x, \Delta y$ , and  $\mu$  are fixed, using the definition of  $r$  in (6), we find that the following restriction on the time-step  $\Delta t$  must be maintained in order to guarantee convergence of GVF:

$$\Delta t \leq \frac{\Delta x \Delta y}{4\mu} \tag{7}$$

The intuition behind this condition is revealing. First, convergence can be made to be faster on coarser images—i.e., when  $\Delta x$  and  $\Delta y$  are larger. Second, when  $\mu$  is large and the GVF is expected to be a smoother field, the convergence rate will be slower (since  $\Delta t$  must be kept small).

An example of contrast between traditional snake and GVF snake is shown in Fig. 1. Fig.1 (a) shows an image (100×100 pixels) having a concave region. Fig.1 (b) shows the initial border ( $\alpha = 0.5, \beta = 0.0$ ). Fig.1 (c) and (d) shows the border output of traditional snake and GVF snake. Fig.1 (e) and (f) shows the potential force field of two snakes. Because the initial border is far from the true boundary, the active contours cannot converge to the true boundary. Clearly, the capture range of traditional snake is very small and GVF snake has a much larger capture range than traditional snake.

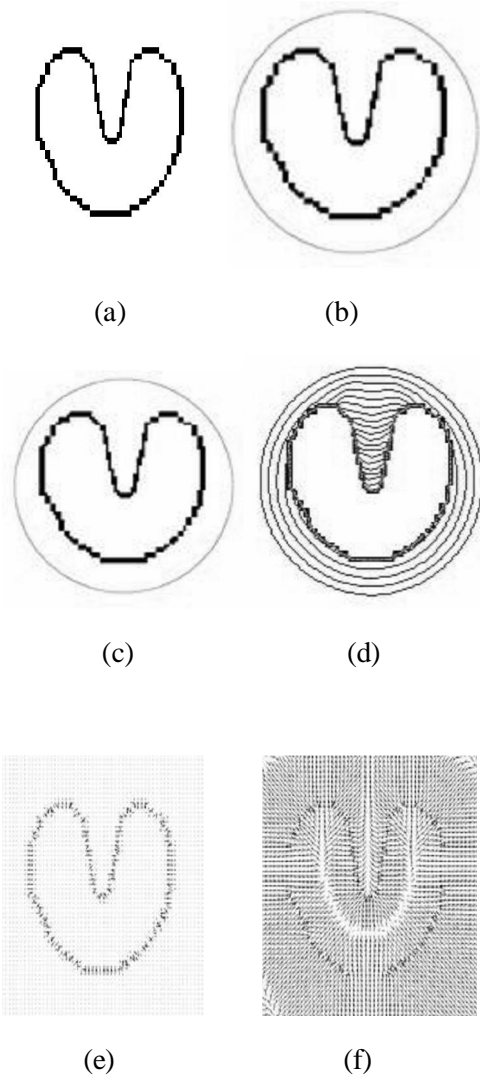


Figure 1. (a) An image having a concave region (b) initial border (c) convergence of traditional snake (d) convergence of GVF snake (e) force field of traditional snake (f) force field of GVF Snake

**Level set:**

In idea of level set method [6,12] ,a contour C is represented by the zero level set which is called a

level set function that of a higher dimensional

function (3Dsurface) with the motion of the curve embedded in the motion of the higher dimensional surface. The motion of the front is matched with the zero level set of a signed distance function H .In the level set method, the curve is represented implicitly

as a level set of a 2D scalar function referred to as the level set function which is usually defined on the same domain as the image. The level set is defined as the set of points that have the same function value. It is worth noting that the level set function is different from the level sets of images, which are sometimes used for image enhancement. The sole purpose of the level set function is to provide an implicit representation of the evolving curve. Level set

function take positive and negative values

outside and inside the contour C. the energy functional e defined by:

$$e(\phi, f_1(x), f_2(x)) = \sum_{i=1}^2 \lambda_i \int_M k_\sigma(x-y) |I(y) - f_i(x)|^2 N_i(\phi(y)) dy \tag{8}$$

Where  $N_1(\phi) = H(\phi)$  and  $N_2(\phi) = 1 - H(\phi)$ ,

k is a Gaussian kernel. The  $f_1(x)$  and  $f_2(x)$  are two values that approximate image intensities in outside and inside of C, respectively. I is input image. Energy functional for contour C that converts to level set formulation written by

$$E(\phi, f_1, f_2) = \sum_{i=1}^2 \lambda_i \int_M dx + \nu \int |\nabla H(\phi(x))| dx \tag{9}$$

where the last term  $\int |\nabla H(\phi(x))| dx$  computes

the length of the zero level contour of that can be

equivalently expressed as the integral  $\int \delta(\phi(x)) |\nabla \phi(x)| dx$

with the Dirac delta function  $\delta(\phi(x))$ , which has often been used in variation level set methods. In practice, the

Heaviside function H in the above energy functional

is approximated by a smooth function  $H_\epsilon$  defined by

$$H_\epsilon(x) = \frac{1}{2} \left[ 1 + \frac{2}{\pi} \arctan\left(\frac{x}{\epsilon}\right) \right] \tag{10}$$

The derivative of  $H_\epsilon$  is

$$\delta_\epsilon(x) = H'_\epsilon(x) = \frac{1}{\pi} \frac{\epsilon}{\epsilon^2 + x^2} \tag{11}$$

By replacing H in (9) with  $H_\epsilon$ , the energy functional  $e$  in (8) is then approximated by

$$(\phi, f_1, f_2)_\epsilon = \sum_{i=1}^2 \lambda_i \int k_\sigma(x-y) |I(y) - f_i(x)|^2 N_i^\epsilon(\phi(y)) dy + \nu \int |\nabla H_\epsilon(\phi(x))| dx \tag{12}$$

As proposed in [14], we introduce a level set regularization term that is necessary for accurate computation and stable level set evolution.

$$\rho(\phi) = \int \frac{1}{2} (|\nabla \phi(x)| - 1)^2 dx \tag{13}$$

Which characterize the deviation of the function

from a signed distance function. Therefore, we

propose to minimize the energy functional

$$\mathcal{F}(\phi, f_1, f_2) = (\phi, f_1, f_2)_\epsilon + \mu \rho(\phi)$$

Where  $\mu$  is a positive constant. To minimize this energy functional, its gradient flow is used as the level set evolution equation in this method. by keeping  $f_1$  and  $f_2$  fixed, the energy functional

( $\phi, f_1, f_2$ ) with respect to  $\phi$  using the standard

gradient descent method by solving the gradient flow equation as follows:

$$\frac{\partial \phi}{\partial t} = -\delta(\phi)(\lambda_1 r_1 - \lambda_2 r_2) + \nu \delta_\epsilon(\phi) \operatorname{div} \left( \frac{\nabla \phi}{|\nabla \phi|} \right) + \mu (\nabla^2 \phi - \operatorname{div} \left( \frac{\nabla \phi}{|\nabla \phi|} \right))$$

Where  $r_1$  and  $r_2$  are the functions

$$r_i(x) = \int k_\sigma(y-x) |I(x) - f_i(y)|^2 dy, \quad i = 1, 2$$

The term  $-\delta(\phi)(\lambda_1 r_1 - \lambda_2 r_2)$  is derived from the data fitting energy, and, therefore, is referred to as the data fitting term. This term plays a key role in this model, since it is responsible for driving the active contour toward object boundaries. The second term

$\operatorname{div} \left( \frac{\nabla \phi}{|\nabla \phi|} \right)$  has a length shortening or

smoothing effect on the zero level contours, which is necessary to maintain the regularity of the contour. This term is called the arc length term. The third

term  $\mu (\nabla^2 \phi - \operatorname{div} \left( \frac{\nabla \phi}{|\nabla \phi|} \right))$  is called a level set

regularization term, since it serves to maintain the regularity of the level set function.

### Image test set

A set of four 3D images is selected to serve as the representative test set as shown in Figure 2 cells is selected from different cancers. In 2007, the American Cancer Society estimated that 559,650 people will die in the United States of cancer in that year alone. This amounts to more than 1,500 people per day [20]. On a positive note, studies show that the five year relative survival rate for all cancers diagnosed has increased to 66% (1996-2000) from 51% (1975-1977). This increase in survival rates is attributed in part to the progress made in detecting certain cancers at an earlier stage. For early detection it is necessary that cells are segmented. Each test image was one of several similar images or image slices in our database and the experiments were comprehensive within The database. The typical

difficulties of image processing presented in the test

set include : blur or weak edge , strong edge near the missing edge , profile contour in overlapping objects, complex contour shape with accentuated protrusions and concavities, in homogeneous interior intensity distribution. These are some of the typical challenges that would fail any simple segmentation schemes.

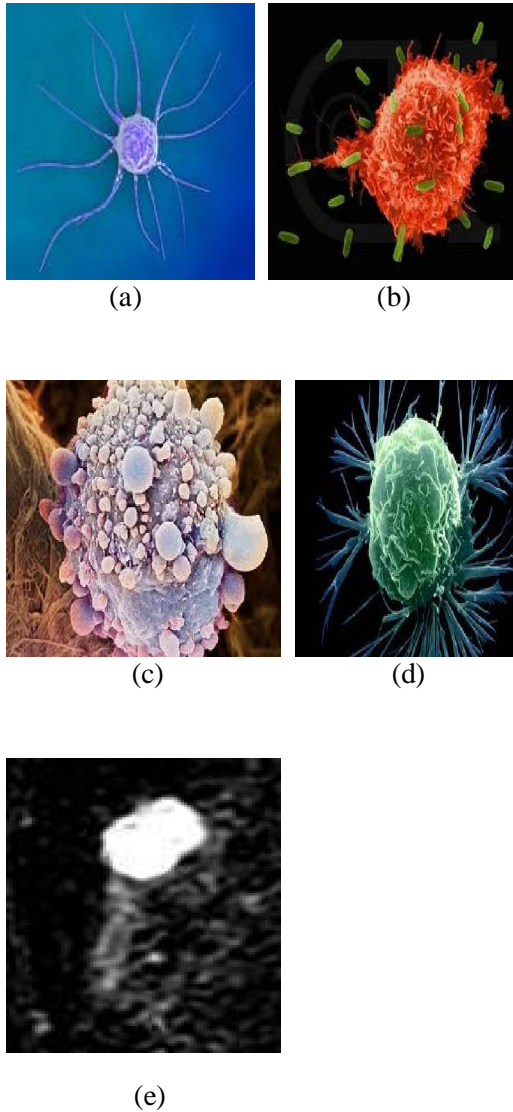


Figure 2. (a) Breast cancer cell. (b) Pancreatic cancer. (c) Cancer cell. (d) Breast cancer cell SME (e) breast cancer tumor

### Implementation and Experimental results

GVF snake has been proposed to deal with the traditional snake's problems of short capture range and inability to track at boundary concavity. But GVF cannot capture object contours in some complicated images. In order to compare the segmentation performance between level set and GVF snake, we run matlab code and show results in this section. Usually, the GVF snake method only works when the boundary is clear and complete because of the boundary detector term and the initial contour that is located close to object, this problem is shown in figure3, tumor is not segmented when initial contour is far away from object. GVF model cannot work in complicated images too (see figure4 and figure5). In figure4 is shown initial contour and segmented cell.

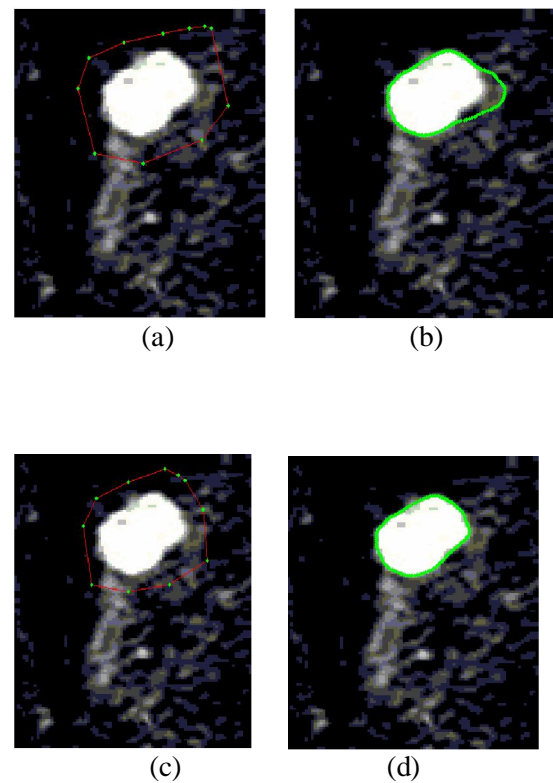


Figure 3. (a) Far away initial contour (b) segmented tumor (c) closed initial contour (d) segmented tumor

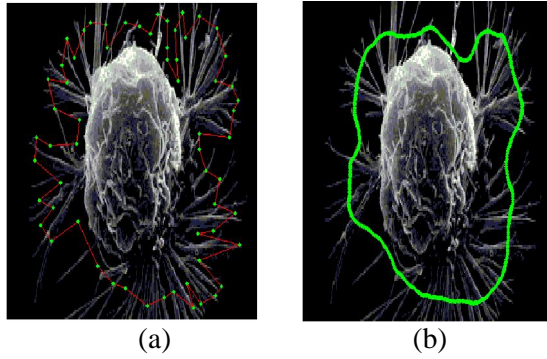


Figure4. (a) Initial contour (b) segmented breast cancer's cell

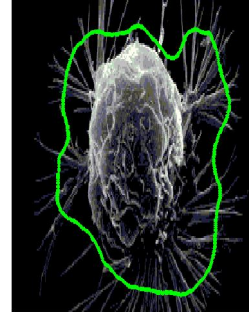
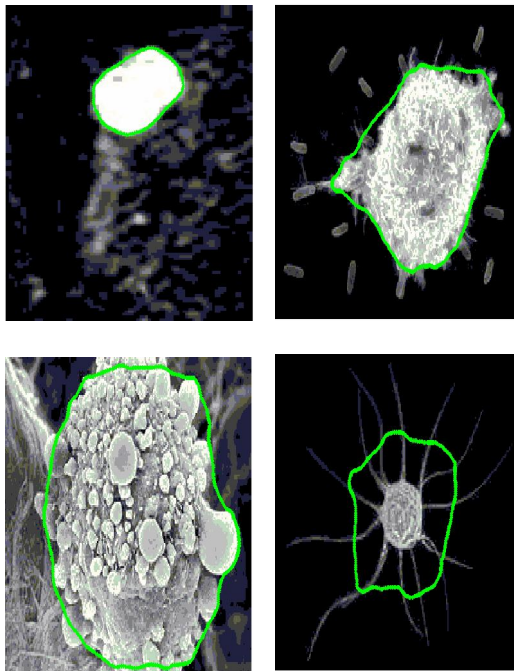
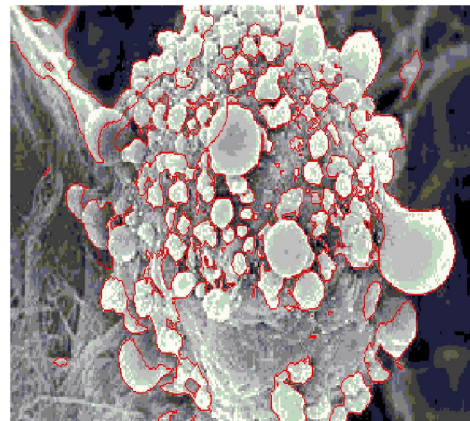
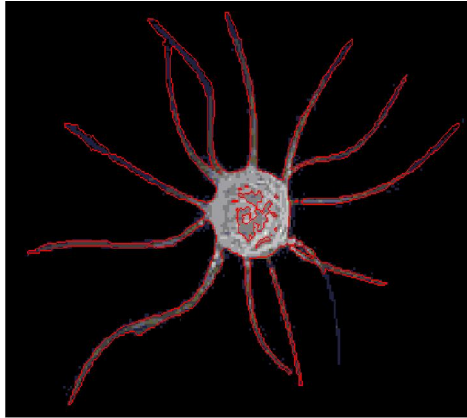


Figure 5 .segmented cells with GVF snake

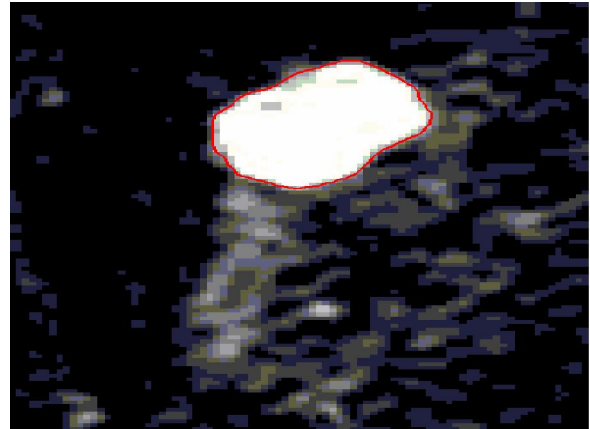
Level set method has been tested with images too. Unless otherwise specified, we use the following parameters in this paper:  $\epsilon = 3$ ,  $\lambda = 1$ ,  $\mu = 2$ , time step  $\Delta t = 0.1$ ,  $\mu = 1$ , and  $\sigma = 0.02 * 255 * 255$ . We use relatively small scale parameter  $\epsilon$  for the experiments in this section. In general, method with a smaller scale  $\epsilon$  can produce more accurate location of the object boundaries, while it is more independent of the location of the initial contour when a larger  $\epsilon$  is used .figure 6 shows the segmentation results by level set method.



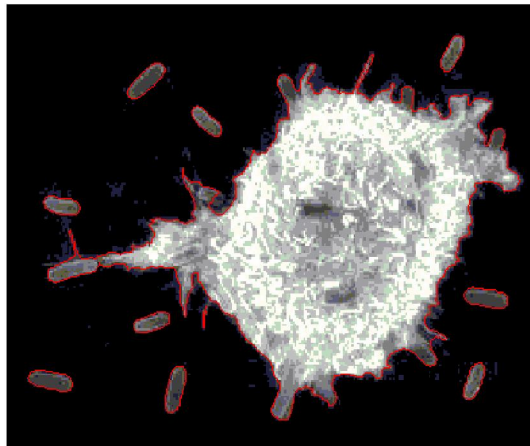
(a) Breast cancer cell



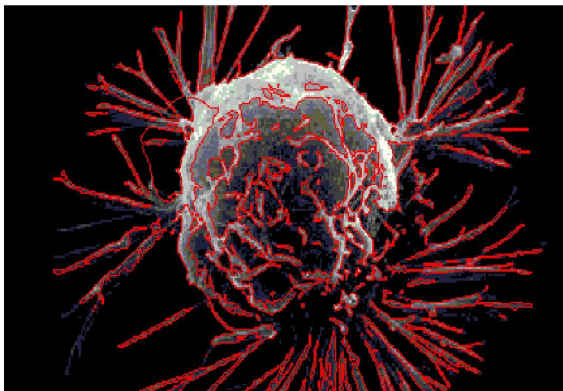
(b) Pancreatic cancer



(e) Breast cancer tumor



(c) Cancer cell



(d) Breast cancer cell, SME,

Figure6. Segmented cells with level set method

**Conclusion:**

GVF is used in image segmentation, but when the image does not have clear boundary or divided to multipart, GVF cannot segment the image, whenever, Level set is a method that can change the topology and segment complicated image. In this paper we demonstrated superior performance of level set in image segmentation compared with GVF.

**References:**

[1] Osher, S., Sethian, J.A. Fronts propagating with curvature dependent speed: algorithms based on Hamilton Jacobi formulations. *J.Comp.Phys.* 1988. 79:12-49.

[2] Malladi, R., Sethian, J., Vemuri, B. Shape modeling with front propagation. *IEEE Trans. Pattern Anal. Machine Intell.* 1995. 17(2):158-171.

[3] Kass, M., Witkin, A., Terzopoulos, D. Snakes: active contour models. *Int. J.Comput.Vis.* 1988. 1 (4): 321-331

[4] Paragios, N., Deriche, R. Geodesic active regions and level set methods for supervised texture segmentation. *Int. J. Comput. Vis.* 2002. 46: 223-247

[5] Xu, C., Prince, J. Snakes, shapes, and gradient vector flow. *IEEE Trans. Image Process.* 1998. 7(3): 359-369

[6]Li, C., Kao, C., Gore, J., Ding, Z. Minimization of Region-Scalable Fitting Energy for Image Segmentation, IEEE Trans. Image Process. 2008. 17(10): 1940-1949.

[7] Jain, A.K., 1989. Fundamentals of Digital Image Processing. Englewood Cliffs, NJ: Prentice-Hall.

[8] Horn, B.K.P., Schunck, B.G. Determining optical flow. Artif. Intell. 1981. 17: 185–203.

[9] Gupta, S.N., Prince, J.L. Stochastic models for DIV-CURL optical flow methods. IEEE signal Processing Lett. 1996. 3: 32–35.

[10] Courant, R., Hilbert, D. Methods of mathematical Physics. New York: Interscience. 1953. 1.

[11] Charles, A.H., Porsching, T.A. Numerical Analysis of Partial Differential Equations. Englewood Cliffs, NJ: Prentice-Hall. 1990.

[12]Li, C., Xu, C., GUI, C., Fox, MD. Level set evolution without reinitialization: A new variational Formulation. In the Proceedings of the IEEE Conference Computer Vision and Pattern Recognition. 2005.

[13]Li, C. Active contours with local binary fitting energy. In the Proceedings of the IMA Workshop on New Mathematics and Algorithms for 3-D Image Analysis. 2006.

[14]Li, C., Kao, C., Gore, J., Ding, Z. Implicit active contours driven by local binary fitting energy. In the Proceedings of the IEEE Conference Computer Vision and Pattern Recognition. 2007.

[15]Li, S., Wang, L., Kao, C., Ding, Z., Gore, J. Brain MR image segmentation by minimizing scalable Neighborhood intensity fitting energy: A multiphase level set approach. In the Proceedings of the ISMRM conference. 2008.

[16] Ganjdanesh, Y., Manjili, Y.S., Vafaei, M., Zamanizadeh, E., Jahanshahi, E. Fuzzy fault detection and diagnosis under severely noisy conditions using feature-based approaches. In the Proceedings of the American control conference. 2008.

[17] Caselles, V., Kimmel, R., Sapiro, G. Geodesic active contours. Int. J. Comput. Vis. 1997. 22 (1): 61–79.

[18] Zhu, S.C., Yuille, A. Region competition: unifying snakes, region growing, and Bayes / MDL formulti band image segmentation. IEEE Trans. Pattern Anal. Machine Intell. 1996. 18(9): 884–900.

[19] Chan, T.F., Vese, L.A. Active contour without edges. IEEE Trans. Image Process. 2001. 10: 266–277.

[20] American Cancer Society. Cancer Facts & Figures 2007. Atlanta: American Cancer Society. 2007

12/8/2010